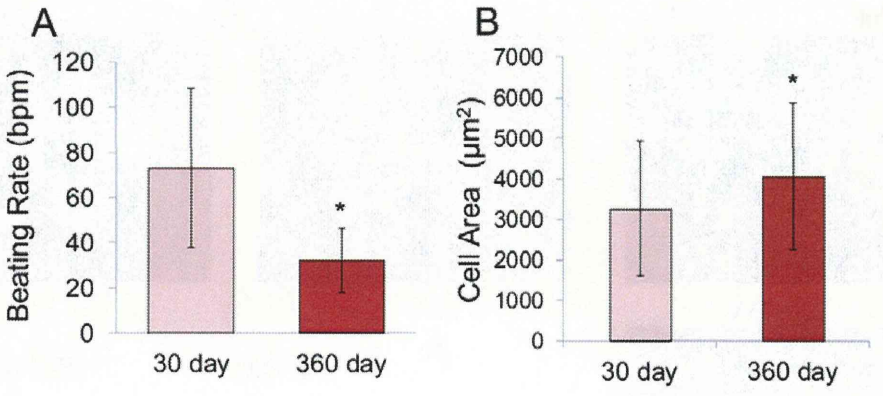

Figure 1. Comparison of human-induced pluripotent stem cell-derived cardiomyocytes (hiPSC-CMs) at 30 and 360 days after cardiac differentiation. (**A**) The rate of beating (beats/min [bpm]) of embryoid bodies (EBs) at 30 days was significantly higher than that of 360-day EBs (73.2±34.9 bpm vs. 32.2±14.2 bpm, P<0.0001). (**B**) Size of hiPSC-CMs increased significantly after long-term culture (3,277.4±1,679.5 μm^2 vs. 4,067.9±1,814.6 μm^2, P=0.01). *P<0.05 vs. 30-day.

maturation process and establish a protocol for creating homogeneous mature iPSC-CMs.

In this study, we investigated the ultrastructural, immunocytological, and gene expression changes of hiPSC-CMs in a long-term 2D culture. Here, we first report that mature sarcomeric structures with M-bands were detected only in 360-day hiPSC-CMs, which might be associated with lower expression levels of M-band-specific proteins compared with adult heart cells.

Methods

Culture of hiPSC and CM Differentiation

The hiPSC line 201B7 was retrovirally transfected with Oct3/4, SOX-2, Klf4, and c-Myc.[1,9] These lines displayed all the defining parameters[1] and the hiPSCs were maintained as described.[15]

We differentiated hiPSC-CMs as embryoid bodies (EBs).[16,17] In brief, hiPSCs aggregated to form EBs, and were cultured in suspension for 8 days. On day 8, the EBs were plated onto fibronectin-coated dishes and for the first 20 days, we followed the protocol as described previously.[16,17] Cultures were maintained in a 5% CO_2, 5% O_2, 90% N_2 environment for the first 12 days and then transferred into a 5% CO_2/air environment for the remainder of the culture period. At 20 days after cardiac differentiation, EBs were maintained in culture DMEM/F12 supplemented with 2% fetal bovine serum, 2 mmol/L L-glutamine, 0.1 mmol/L non-essential amino acids, 0.1 mmol/L β-mercaptoethanol, 50 U/ml penicillin, and 50 μg/ml streptomycin.[3] The medium was renewed every 2–3 days.

Immunocytochemistry

For immunostaining, single cells were isolated from microdissected 30- and 360-day-old beating EBs using collagenase B (Roche) and trypsin EDTA (Nacalai Tesque). The cells were plated onto fibronectin-coated dishes for 3 days to allow attachment. The cells were fixed in 4% paraformaldehyde and permeabilized in 0.2% Triton X-100 (Nacalai Tesque). The samples were stained with the following primary antibodies: rabbit polyclonal anti-cardiac troponin I (cTnI) (1:200; Santa Cruz), mouse monoclonal anti-myosin light chain 2a (MLC2a) (1:200; Synaptic Systems), rabbit polyclonal anti-myosin light chain 2v (MLC2v) (1:100; Proteintech Group), mouse monoclonal anti-βIII tubulin (1:100, Promega), mouse monoclonal anti-fibroblast (1:100, Acris Antibodies), and mouse monoclonal anti-human smooth muscle actin (1:100, Dako). We used the appropriate secondary antibodies: donkey anti-rabbit Alexafluor 594 (1:500, Invitrogen) and donkey anti-mouse Alexafluor 488 (1:500, Invitrogen). The nuclei were stained with DAPI (1:2000, Wako). The specimens were observed under a fluorescence microscope, Biozero BZ-9000 (Keyence), and the areas of cTnI-positive cells were calculated using a BZ-II analyzer (Keyence).

Transmission Electron Microscopy (TEM)

TEM was performed on 14-, 30-, 60-, 90-, 180-, and 360-day old EBs derived from hiPSC-CMs. EBs were microdissected and fixed for 1 h in 2% glutaraldehyde at 4°C in phosphate-buffered saline (PBS). All sections were treated with OsO_4 (1% for 1 min, and 0.5% for 20 min at 4°C) in PBS, dehydrated in ethanol and propylene oxide, and embedded in Luveak 812 (Nacalai Tesque). Ultrathin sections were cut with an ultramicrotome (Leica, Heidelberg, Germany) and observed with TEM (H-7650; Hitachi). All stages of EBs were examined in triplicate.

Analysis of mRNA Expression by Real-Time Quantitative Polymerase Chain Reaction (qPCR)

Total RNA was isolated using TRIzol Reagent (Invitrogen) from 20 to 30 EBs microdissected from 30-, 90-, 180-, and 360-day-old hiPSC-CMs, and treated with TURBO DNA-free Kit (Applied Biosystems). Total RNA from human heart tissue (left ventricle, left atrium, and fetal heart) was also reverse transcribed into complementary DNA (cDNA) for comparison. cDNA was synthesized from 1 μg of total RNA, in a total volume of 20 μl, using oligo $(dT)_{18}$ primer with Transcriptor First Strand cDNA Synthesis Kit (Roche). The PCR-related primers are detailed in **Table S1**. The real-time qPCR was performed using power SYBR Green PCR Master Mix (Applied Biosystems) for 6 samples. The expression of genes of interest was normalized to that of *GAPDH*. Relative quantification was calculated according to the $\Delta\Delta C_T$ method. The changes in gene expression levels were compared with those of hiPSC-

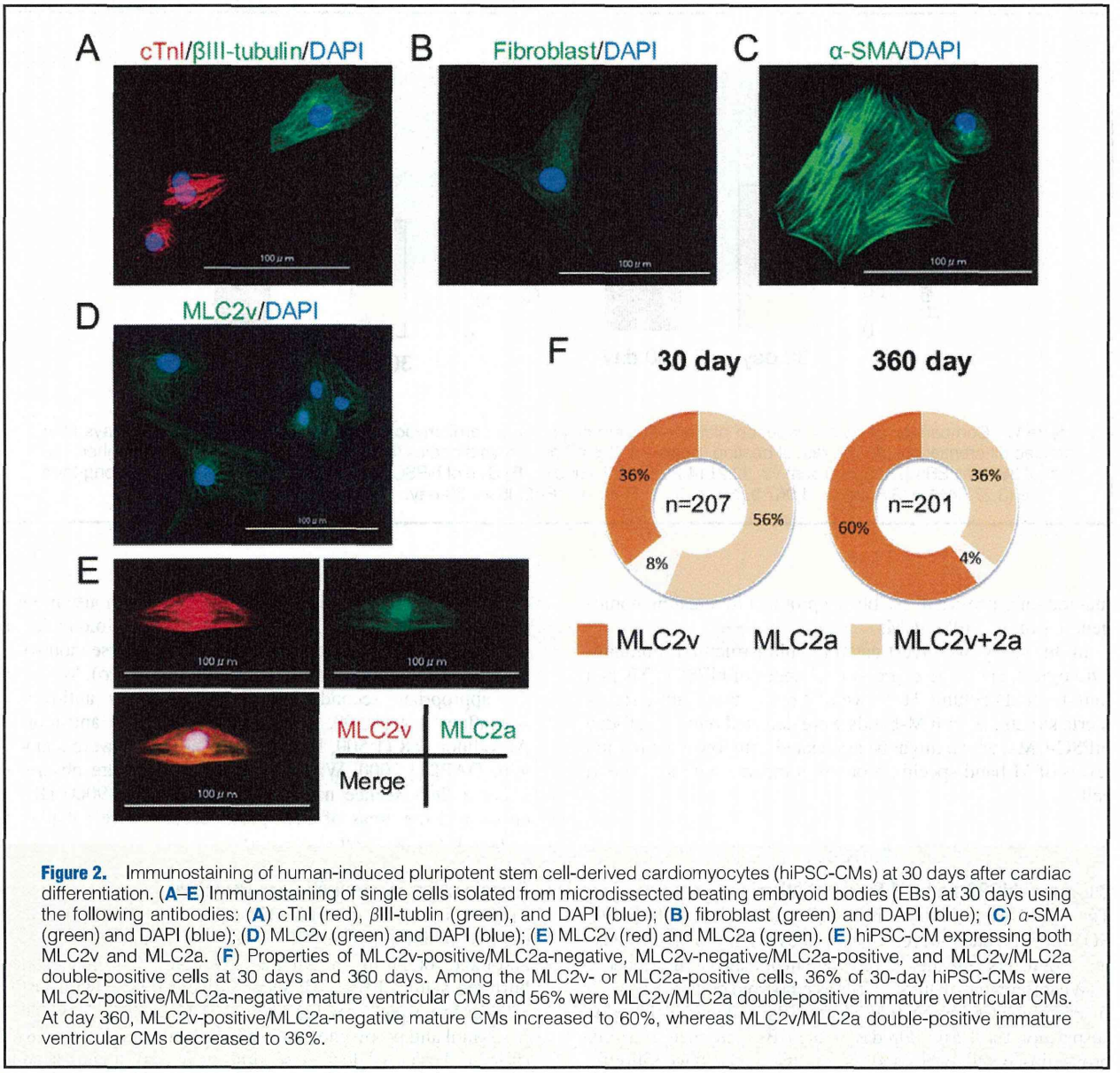

Figure 2. Immunostaining of human-induced pluripotent stem cell-derived cardiomyocytes (hiPSC-CMs) at 30 days after cardiac differentiation. (**A–E**) Immunostaining of single cells isolated from microdissected beating embryoid bodies (EBs) at 30 days using the following antibodies: (**A**) cTnI (red), βIII-tublin (green), and DAPI (blue); (**B**) fibroblast (green) and DAPI (blue); (**C**) α-SMA (green) and DAPI (blue); (**D**) MLC2v (green) and DAPI (blue); (**E**) MLC2v (red) and MLC2a (green). (**E**) hiPSC-CM expressing both MLC2v and MLC2a. (**F**) Properties of MLC2v-positive/MLC2a-negative, MLC2v-negative/MLC2a-positive, and MLC2v/MLC2a double-positive cells at 30 days and 360 days. Among the MLC2v- or MLC2a-positive cells, 36% of 30-day hiPSC-CMs were MLC2v-positive/MLC2a-negative mature ventricular CMs and 56% were MLC2v/MLC2a double-positive immature ventricular CMs. At day 360, MLC2v-positive/MLC2a-negative mature CMs increased to 60%, whereas MLC2v/MLC2a double-positive immature ventricular CMs decreased to 36%.

CMs at 30-day differentiation. The fold change is expressed as mean±SEM.

Statistical Analysis

All values are presented as mean±SEM. Statistical significance was evaluated by Student's t-test for 2 groups or 1-way analysis of variance followed by Tukey test for comparisons of multiple groups. Differences with $P<0.05$ were considered statistically significant.

Results

Long-Term Maintenance of hiPSC-CMs

Areas of spontaneous beating became visible as early as day 8 after differentiation, and kept beating for more than 360 days (**Movie S1**). The beating rate of 30-day-old EBs (n=42) was significantly higher than that of 360-day-old EBs (n=41; 73.2±34.9 beats/min vs. 32.2±14.2 beats/min, $P<0.0001$) (**Figure 1A**). The size of dispersed hiPSC-CMs increased significantly after long-term culture as measured by their cell area (3,277.4±1,679.5 μm^2 vs. 4,067.9±1,814.6 μm^2, $P=0.01$) (**Figure 1B**).

Immunostaining Analysis of Beating EBs at 30 and 360 Days After Cardiac Differentiation

Immunostaining of single cells isolated by microdissected beating EBs detected cells positive not only for cTnI, MLC2v, and MLC2a, but also βIII-tubulin, fibroblasts, and α-SMA, suggesting the existence of neural cells, fibroblast-like cells, and vascular smooth muscle cells in the beating EBs as well as CMs (**Figures 2A–E**).

Among randomly selected single cells isolated from 30- (n=213) and 360-day-old (n=191) beating EBs, 61% and 64%, respectively, were positive for cTnI. Double immunostaining with anti-MLC2v and anti-MLC2a antibodies revealed that among the MLC2v- or MLC2a-positive cells, 36% were MLC2v-positive/MLC2a-negative, 8% were MLC2v-negative/

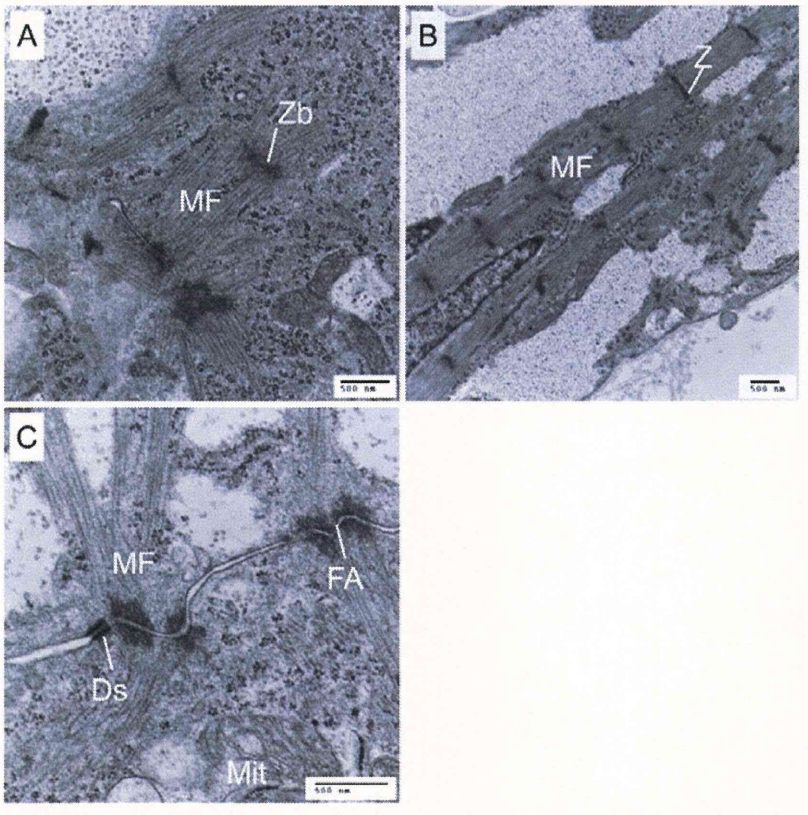

Figure 3. Transmission electron microscopy images of human-induced pluripotent stem cell-derived cardiomyocytes (hiPSC-CMs) at 14 days after cardiac differentiation. (**A**) hiPSC-CMs at 14 days contained myofibrils (MF) that lacked alignment or organized sarcomeric pattern. Scattered condensed Z-bodies (Zb) were also confirmed. (**B**) In some areas, a more developed pattern was noted in which myofibrils (MF) were held between a few of the Z-bands (Z). (**C**) CMs connected by desmosomes (Ds) and fascia adherens (FA) even at this early stage. Mitochondria (Mit) can be seen.

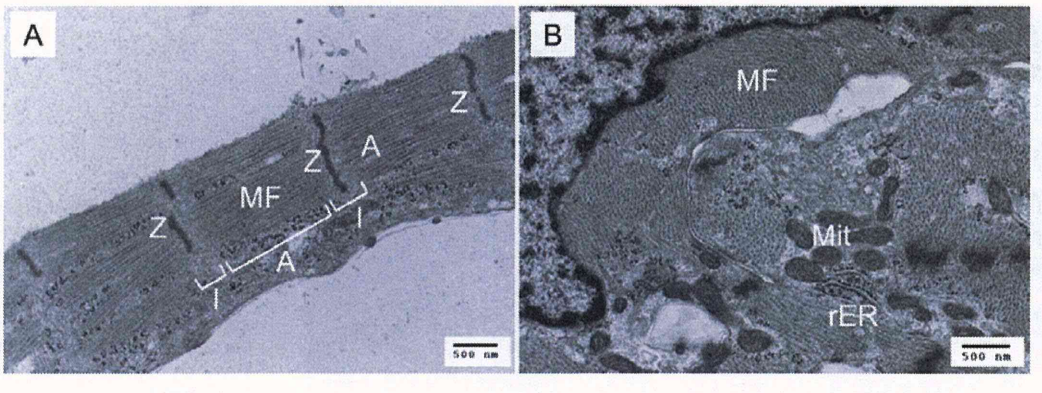

Figure 4. Transmission electron microscopy images of human-induced pluripotent stem cell-derived cardiomyocytes (hiPSC-CMs) at 30 days after cardiac differentiation. (**A**) hiPSC-CMs at 30 days appeared to be packed between parallel Z-bands. Some myofibrils (MF) showed A- (A) and I-bands (I). (**B**) Transverse section of sarcomere and rough endoplasmic reticulum (rER). Mitochondria (Mit) can be seen.

MLC2a-positive, and 56% were MLC2v/MLC2a double-positive CMs at 30-day differentiation. By day 360, MLC2v-positive/MLC2a-negative CMs increased to 60%, whereas MLC2v/MLC2a double-positive immature ventricular CMs decreased to 36% (**Figure 2F**).

Ultrastructural Analysis of hiPSC-CMs at 14-, 30-, 60-, 90-, 180-, and 360-Day Differentiation

hiPSC-CMs at 14-day differentiation contained myofibrils that lacked alignment or organized sarcomeric pattern, and were distributed diffusely in the cytoplasm in a disorganized fashion. Scattered patterns of condensed Z-bodies were also confirmed. However, in some areas, a more developed pattern was

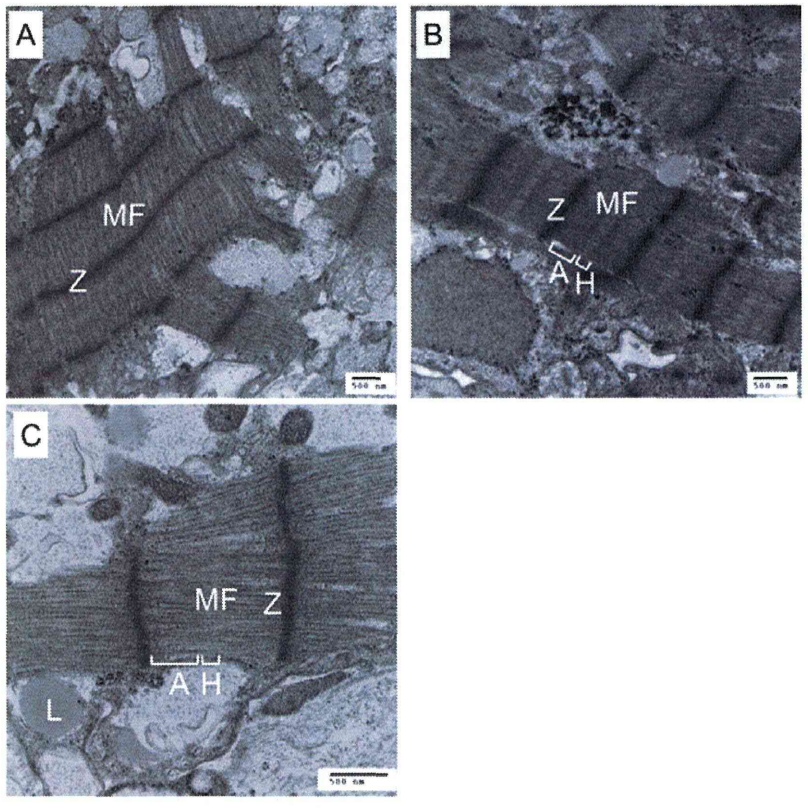

Figure 5. Transmission electron microscopy images of human-induced pluripotent stem cell-derived cardiomyocytes (hiPSC-CMs) at 60 (**A**), 90 (**B**), and 180 days (**C**) after cardiac differentiation. Between 60- and 180-day differentiation, ultrastructural maturation continued and formation of H-bands (H) can be seen. However, even at 180-day differentiation, M-bands are not apparent. Lipid droplets (L) can be seen in (**C**).

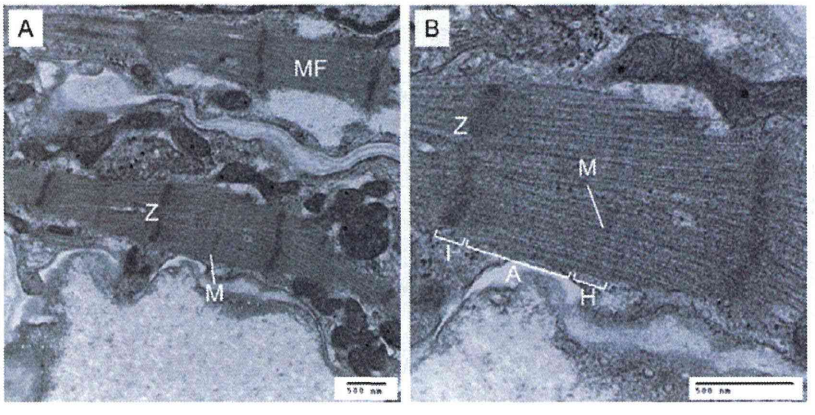

Figure 6. Transmission electron microscopy images of human-induced pluripotent stem cell-derived cardiomyocytes (hiPSC-CMs) at 360 days after cardiac differentiation. (**A**,**B**) In addition to discrete A-, H-, I-, and Z-bands, M-bands (M) are also noted in a minority of the cells within the sarcomeres.

noted in which myofibrils were held between a few of the Z-bands (**Figure 3**). However, A-, H-, I-, and M-bands were not recognized. CMs were connected by desmosomes and fascia adherens at this early stage.

At 30-day differentiation, nascent myofibrils decreased and appeared to be packed between Z-bands. Parallel Z-bands were demonstrated to confine the myofibrils in the typical sarcomeric pattern. Some myofibrils showed A- and I-bands. However, they still lacked the formation of H-, and M-bands (**Figure 4**). Mitochondria and rough endoplasmic reticulum were also noted, as previously reported.[13]

Between 60- and 90-day differentiation, ultrastructural maturation continued and formation of H-bands could be observed. However, even at 180-day differentiation, M-bands could not be detected (**Figure 5**).

Finally, at 360-day differentiation, in addition to discrete A-, H-, I-, and Z-bands, M-bands were first noted in a minority of the cells within the sarcomeres (**Figure 6**). Myofibrils appeared to be tightly packed and distributed in an oriented fashion. The amount of sarcomeric structure in a single CM continued to increase, but was still scarce compared with an adult CM. Even at this stage, different degrees of organization

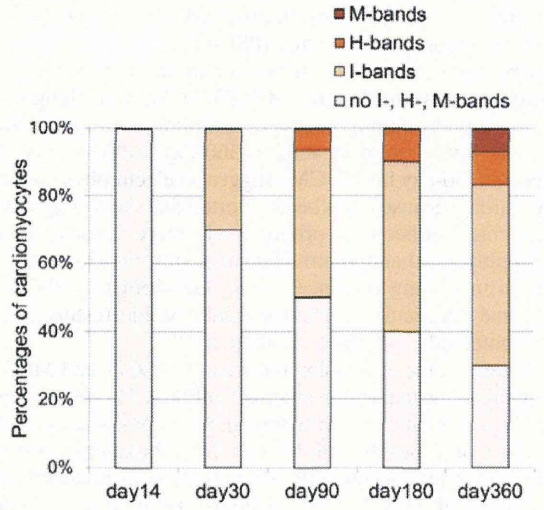

Figure 7. Percentages of the cardiomyocytes (CMs) having I-, H-, and M-bands at 14, 30, 90, 180, 360 days after cardiac differentiation. The amount of CMs with I- and H-bands increased through the long-term culture and M-bands were first noted in 360-day CMs.

existed simultaneously in the same EB.

We evaluated 30 CMs with sarcomeres on randomly selected electron micrographs to assess the maturation process of sarcomeres quantitatively. **Figure 7** shows the percentages of CMs having I-, H-, and M-bands at 14-, 30-, 90-, 180-, 360-day differentiation.

Expression of Cardiac-Specific Genes

Leucine-rich repeat-containing protein 39 (*LRRC39*), myomesin 1 (*MYOM1*), and 2 (*MYOM2*), components of M-bands,[18] increased at 360-day differentiation compared with 30-day differentiation, supporting the observation of M-band formation in 360-day hiPSC-CMs (**Figure 8**). However, the expression levels of the M-band-specific proteins in the hiPSC-CMs were lower compared with those of the adult heart. The expression of cardiac troponin-T (*cTnT*), myosin heavy chain 6 (*MYH6*), myosin heavy chain 7 (*MYH7*), and myosin regulatory light chain 2 (*MYL2*) also increased after the 1-year culture. However, the expression levels of cardiac-specific genes in the hiPSC-CMs were also considerably lower than those in the adult heart left ventricle or left atrium, and in the fetal heart. The expression levels of gap junction α-1 protein were significantly decreased in 180-day and 360-day hiPSC-CMs compared with 30-day hiPSC-CMs.

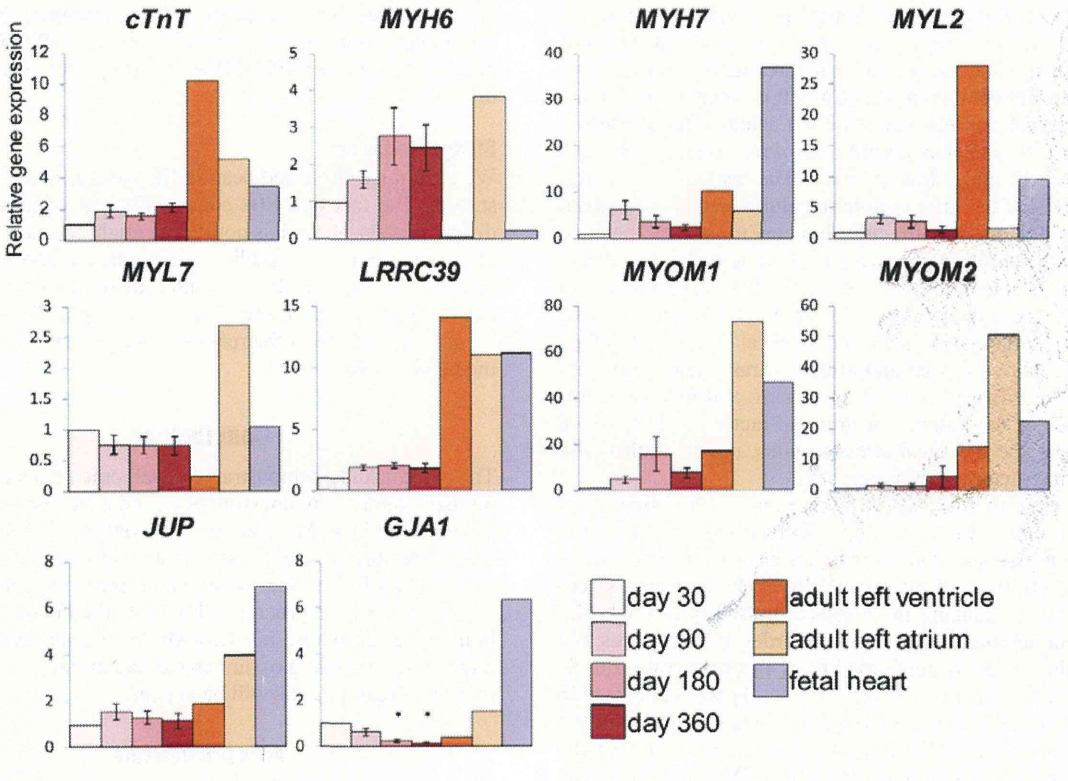

Figure 8. Real-time quantitative polymerase chain reaction analyses for *cTnT*, *MYH6*, *MYH7*, *MYL2*, *MYL7*, *LRRC39*, *MYOM1*, *MYOM2*, *JUP*, and *GJA1* expression in beating embryoid bodies (EB) from human-induced pluripotent stem cell-derived cardiomyocytes (hiPSC-CMs) at 30, 90, 180, and 360 days, in the adult left ventricle, adult left atrium, and fetal heart. The changes in gene expression levels were compared with those of hiPSC-CMs at 30-day differentiation. *cTnT*, cardiac troponin-T; *MYH6*, myosin heavy chain 6; *MYH7*, myosin heavy chain 7; *MYL2*, myosin regulatory light chain 2; *MYL7*, myosin regulatory light chain 7; *LRRC39*, leucine-rich repeat-containing protein 39; *MYOM1*, myomesin 1; *MYOM2*, myomesin 2; *JUP*, junction plakoglobin; *GJA1*, gap junction α-1 protein. *P<0.05 vs. 30-days EBs.

Discussion

In this study, we demonstrated that hiPSC-CMs continue to mature through a 1-year culture. This is the first report of the feasibility of 1-year 2D culture of hiPSC-CMs and description of the sarcomeric maturation process represented by the emergence of M-bands and the increase in the cardiac-specific gene expressions.

So far, the reported ultrastructure of hiPSC-CMs has been immature and their maturation process remained unknown.[4,13,14] Human embryonic stem cell-derived cardiomyocytes (hESC-CMs) are reported to follow a roughly similar maturation process to that reported both in vivo and in an in-vitro murine ES model.[19–24] The hiPSC-CMs in the present study showed a similar maturation process to that of hESC-CMs.[25] At first, narrow, diffusely distributed, and frequently not well aligned myofibrils, resembling those of hiPSC-CMs at 14 days, developed into sarcomeres with clear band patterns including the Z-, I-, and A-bands, responding to hiPSC-CMs at between 30 and 90 days, and ultimately resulted in the generation of well-designed sarcomeres with A-, H-, I-, and M-bands. The ultrastructural findings of hiPSC-CMs in the literature now available relate to around 30 days of differentiation, and only Z- and I-bands have been visible.[4,13,14] In our study, the 30-day hiPSC-CMs similarly showed only Z- and I-bands, not H- or M-bands. Notably, we are the first to find that only 360-day hiPSC-CMs, not 180-day hiPSC-CMs, show a mature sarcomeric structure with M-bands. However, even at 360-day differentiation, different degrees of organization patterns existed simultaneously in the same EB and homogeneous maturation was not confirmed. Our 1-year culture system was able to confirm more mature sarcomeric structures than previously reported, but still not that of adult CMs. It is reported that human CMs derived from fetal hearts do not achieve full ultrastructural maturity and that myofibrillar development continues throughout the entire fetal period.[22] The insufficient maturation of hiPSC-CMs after long-term culture could be explained by several factors. In vitro culturing conditions lack the presence of adjacent non-myocyte proliferating cells, which play an important role in the maturation of CMs via paracrine and humoral signals in vivo. In addition, the CMs grown in the absence of hemodynamic workload typical of in vivo working CMs are reported to lack appropriate ultrastructural development.[26] The differences between in vitro and in vivo conditions, such as the absence of humoral factors and organized mechanical and electrical stress in vitro, might result in delayed ultrastructural maturation.

In electron micrographs of the sarcomere, the M-band appears as a series of parallel electron-dense lines in the central zone of the A-band. The M-band has been reported to play a role not only in mechanical stability in the activated sarcomere, such as reducing the intrinsic instability of thick filaments and helping titin to maintain order in sarcomeres, but also in the biomechanical conditions in contracting muscle such as stress sensing.[27] M-band formation was confirmed in the latest stage and has been considered the endpoint of myofibrillar maturation.[18,21] The lower expression levels of the M-band-specific proteins in the hiPSC-CMs compared with the adult heart might be associated with the delayed appearance of M-bands. Maturation of iPSC-CMs is critical for their application in regenerative medicine, as well as for investigating the mechanisms underlying inherited cardiac diseases. Techniques to promote the maturation of ESC-CMs, such as 3D culture methodology,[28] electric stimulation,[29] and coculture with non-cardiomyocytes[30] may be applicable to iPSC-CMs to overcome the problem, although it has not been fully investigated in hiPSC-CMs. Improved methods are needed to produce homogeneous, mature iPSC-CMs.

In addition to ultrastructural maturation, there was a significant increase in the size of hiPSC-CMs after long-term culture, supporting the process of morphological maturation. Also, the lower rate of beating of 360-day hiPSC-CMs compared with 30-day hiPSC-CMs suggested electrophysiological maturation, because it has been reported that the resting membrane potential becomes progressively more negative in the developing atrial and ventricular myocytes, which correlates with an increasing presence of I_{K1}, and ultimately, the fetal atrial and ventricular myocytes exhibit stable resting membrane potentials with little automaticity.[31]

Changes in the expression patterns of MLC2v and MLC2a occur during the maturation process.[32] hiPSC-CMs were thought to be immature and similar to human fetal CMs because of the presence of a number of MLC2v/MLC2a double-positive CMs.[33] Our immunostaining analysis demonstrated that the percentage of MLC2v/MLC2a double-positive hiPSC-CMs decreased after long-term culture, accompanied by an increase in MLC2v-positive/MLC2a-negative hiPSC-CMs, suggesting maturing of the ventricular-type CMs.

This study also showed for the first time, changes in the expression levels of cardiac-specific genes and genes related to intercalated discs throughout the 1-year culture. The cardiac-specific genes tended to increase during 1-year culture, supporting the maturation process of hiPSC-CMs. The connexin (gap junction proteins) are reported to be more abundant in the neonate than the adult.[34] The significant decrease in *GJA1* expression levels in 180- and 360-day hiPSC-CMs compared with 30-day hiPSC-CMs also suggested maturation of hiPSC-CMs.

Study Limitations

We used microdissected beating EBs for the gene expression studies. The fact that EBs contain CMs at various stages of differentiation, as well as non-CMs, might obscure the results of the gene expression studies. We conducted immunostaining analysis of single cells from microdissected beating EBs 3 days after enzymatic dispersion, which might allow non-CMs to increase and affect the results of the percentage of CMs in the beating EBs.

Conclusions

The current study demonstrated developmental changes in the ultrastructural, immunocytological, and gene expression properties of hiPSC-CMs. Our results confirmed mature sarcomeric structure with M-band formation in long-term culture of hiPSC-CMs for the first time, which provides a new insight into the maturation process of hiPSC-CMs. For application of homogeneous mature hiPSC-CMs in regenerative medicine and in vitro modeling of human cardiac diseases, further maturation of cardiac cells will be needed.

Acknowledgments

We thank Aya Umehara, Masako Tanaka, Kyoko Yoshida, and the Division of Electron Microscopic Study, Center for Anatomical Studies, Kyoto University Graduate School of Medicine for technical assistance.

Sources of Funding

This work was supported by research grants from the Ministry of Education, Culture, Science, and Technology of Japan (T.M. and M.H.), Suzuken Memorial Foundation (T. Kimura), Fujiwara Memorial Foundation

(T.M.), the Uehara Memorial Foundation (M.H.), and health science research grants from the Ministry of Health, Labor and Welfare of Japan for Clinical Research on Measures for Intractable Diseases (T.M. and M.H.).

Disclosures

None.

References

1. Takahashi K, Tanabe K, Ohnuki M, Narita M, Ichisaka T, Tomoda K, et al. Induction of pluripotent stem cells from adult human fibroblasts by defined factors. *Cell* 2007; **131:** 861–872.
2. Zhang J, Wilson GF, Soerens AG, Koonce CH, Yu J, Palecek SP, et al. Functional cardiomyocytes derived from human-induced pluripotent stem cells. *Circ Res* 2009; **104:** e30–e41.
3. Moretti A, Bellin M, Welling A, Jung CB, Lam JT, Bott-Flügel L, et al. Patient-specific induced pluripotent stem-cell models for long-QT syndrome. *N Engl J Med* 2010; **363:** 1397–1409.
4. Novak A, Barad L, Zeevi-Levin N, Shick R, Shtrichman R, Lorber A, et al. Cardiomyocytes generated from $CPVT^{D307H}$ patients are arrhythmogenic in response to β-adrenergic stimulation. *J Cell Mol Med* 2012; **16:** 468–482.
5. Choi SH, Jung SY, Kwon SM, Baek SH. Perspectives on stem cell therapy for cardiac regeneration. *Circ J* 2012; **76:** 1307–1312.
6. Zwi L, Caspi O, Arbel G, Huber I, Gepstein A, Park IH, et al. Cardiomyocyte differentiation of human-induced pluripotent stem cells. *Circulation* 2009; **120:** 1513–1523.
7. Germanguz I, Sedan O, Zeevi-Levin N, Shtrichman R, Barak E, Ziskind A, et al. Molecular characterization and functional properties of cardiomyocytes derived from human inducible pluripotent stem cells. *J Cell Mol Med* 2011; **14:** 38–51.
8. Ma J, Guo L, Fiene SJ, Anson BD, Thomson JA, Kamp TJ, et al. High purity human-induced pluripotent stem cell-derived cardiomyocytes electrophysiological properties of action potentials and ionic currents. *Am J Physiol Heart Circ Physiol* 2011; **301:** H2006–H2017.
9. Tanaka T, Tohyama S, Murata M, Nomura F, Kaneko T, Chen H, et al. In vitro pharmacologic testing using human-induced pluripotent stem cell-derived cardiomyocytes. *Biochem Biophys Res Commun* 2009; **385:** 497–502.
10. Xi J, Khalil M, Shishechian N, Hannes T, Pfannkuche K, Liang H, et al. Comparison of contractile behavior of native murine ventricular tissue and cardiomyocytes derived from embryonic or induced pluripotent stem cells. *FASEB J* 2010; **24:** 2739–2751.
11. Kuzmenkin A, Liang H, Xu G, Pfannkuche K, Eichhorn H, Fatima A, et al. Functional characterization of cardiomyocytes derived from murine induced pluripotent stem cells in vitro. *FASEB J* 2009; **23:** 4168–4180.
12. Jonsson MK, Vos MA, Mirams GR, Duker G, Sartipy P, de Boer TP, et al. Application of human stem cell-derived cardiomyocytes in safety pharmacology requires caution beyond hERG. *J Mol Cell Cardiol* 2012; **52:** 998–1008.
13. Gherghiceanu M, Barad L, Novak A, Reiter I, Itskovitz-Eldor J, Binah O, et al. Cardiomyocytes derived from human embryonic and induced pluripotent stem cells: Comparative ultrastructure. *J Cell Mol Med* 2011; **15:** 2539–2551.
14. Fujiwara M, Yan P, Otsuji TG, Narazaki G, Uosaki H, Fukushima H, et al. Induction and enhancement of cardiac cell differentiation from mouse and human-induced pluripotent stem cells with cyclosporine-A. *PLoS One* 2011; **6:** e16734.
15. Yoshida Y, Takahashi K, Okita K, Ichisaka T, Yamanaka S. Hypoxia enhances the generation of induced pluripotent stem cells. *Cell Stem Cell* 2009; **5:** 237–241.
16. Dubois NC, Craft AM, Sharma P, Elliott DA, Stanley EG, Elefanty AG, et al. SIRPA is a specific cell-surface marker for isolating cardiomyocytes derived from human pluripotent stem cells. *Nat Biotechnol* 2011; **29:** 1011–1018.
17. Yang L, Soonpaa MH, Adler ED, Roepke TK, Kattman SJ, Kennedy M, et al. Human cardiovascular progenitor cells develop from a KDR^+ embryonic-stem-cell-derived population. *Nature* 2008; **453:** 524–528.
18. Will RD, Eden M, Just S, Hansen A, Eder A, Frank D, et al. Myomasp/LRRC39, a heart- and muscle-specific protein, is a novel component of the sarcomeric M-band and is involved in stretch sensing. *Circ Res* 2010; **107:** 1253–1264.
19. Beharvand H, Azarnia M, Parivar K, Ashtiani SK. The effect of extracellular matrix on embryonic stem cell-derived cardiomyocytes. *J Mol Cel Cardiol* 2005; **38:** 495–503.
20. Baharvand H, Piryaei A, Rohani R, Taei A, Heidari MH, Hosseini A. Ultrastructural comparison of developing mouse embryonic stem cell- and in vivo-derived cardiomyocytes. *Cell Biol Int* 2006; **30:** 800–807.
21. Anversa P, Olivetti G, Bracchi PG, Loud AV. Postnatal development of the M-band in rat cardiac myofibrils. *Circ Res* 1981; **48:** 561–568.
22. Kim HD, Kim DJ, Lee IJ, Rah BJ, Sawa Y, Schaper J. Human fetal heart development after mid-term: Morphometry and ultrastructural study. *J Mol Cell Cardiol* 1992; **24:** 949–965.
23. Legat MJ. Sarcomerogenesis in human myocardium. *J Mol Cell Cardiol* 1970; **1:** 425–437.
24. Yu L, Gao S, Nie L, Tang M, Huang W, Luo H, et al. Molecular and functional changes in voltage-gated Na^+ channels in cardiomyocytes during mouse embryogenesis. *Circ J* 2011; **75:** 2071–2079.
25. Snir M, Kehat I, Gepstein A, Coleman R, Itskovitz-Eldor J, Livne E, et al. Assessment of the ultrastructural and proliferative properties of human embryonic stem cell-derived cardiomyocytes. *Am J Physiol Heart Circ Physiol* 2003; **285:** H2355–H2363.
26. Bishop SP, Anderson PG, and Tucker DC. Morphological development of the rat heart growing in oculo in the absence of hemodynamic work load. *Circ Res* 1990; **66:** 84–102.
27. Agarkova I, Perriard JC. The M-band: An elastic web that crosslinks thick filaments in the center of the sarcomere. *Trends Cell Biol* 2005; **15:** 477–485.
28. Ou DB, He Y, Chen R, Teng JW, Wang HT, Zeng D, et al. Three-dimensional co-culture facilitates the differentiation of embryonic stem cells into mature cardiomyocytes. *J Cell Biochem* 2011; **112:** 3555–3562.
29. Chen MQ, Xie X, Wilson KD, Sun N, Wu JC, Giovangrandi L, et al. Current-controlled electrical point-source stimulation of embryonic stem cells. *Cell Mol Bioeng* 2009; **2:** 625–635.
30. Kim C, Majdi M, Xia P, Wei KA, Talantova M, Spiering S, et al. Non-cardiomyocytes influence the electrophysiological maturation of human embryonic stem cell-derived cardiomyocytes during differentiation. *Stem Cells Dev* 2010; **19:** 783–795.
31. He JQ, Ma Y, Lee Y, Thomson JA, Kamp TJ. Human embryonic stem cells develop into multiple types of cardiac myocytes: Action potential characterization. *Circ Res* 2003; **93:** 32–39.
32. Kubalak SW, Miller-Hance WC, O'Brien TX, Dyson E, Chien KR. Chamber specification of atrial myosin light chain-2 expression precedes septation during murine cardiogenesis. *J Biol Chem* 1994; **269:** 16961–16970.
33. Mummery CL, Zhang J, Ng ES, Elliott DA, Elefanty AG, Kamp TJ. Differentiation of human embryonic stem cells and induced pluripotent stem cells to cardiomyocytes: A methods overview. *Circ Res* 2012; **111:** 344–358.
34. Allah EA, Tellez JO, Yanni J, Nelson T, Monfredi O, Boyett MR, et al. Changes in the expression of ion channels, connexins and Ca^{2+}-handling proteins in the sino-atrial node during postnatal development. *Exp Physiol* 2011; **96:** 426–438.

Supplementary Files

Supplementary File 1

Table S1. Primer Sequences Used for Real-Time qPCR Analysis

Supplementary File 2

Movie S1. 360-day-old beating embryoid bodies.

Please find supplementary file(s);
http://dx.doi.org/10.1253/circj.CJ-12-0987

Published in final edited form as:
Circ Cardiovasc Genet. 2013 December 1; 6(6): 624–633. doi:10.1161/CIRCGENETICS.113.000330.

Identification of Chemicals Inducing Cardiomyocyte Proliferation in Developmental Stage-Specific Manner with Pluripotent Stem Cells

Hideki Uosaki, MD, PhD[1], **Ajit Magadum, PhD**[2], **Kinya Seo, PhD**[1], **Hiroyuki Fukushima, MS**[3,4], **Ayako Takeuchi, PhD**[5], **Yasuaki Nakagawa, MD, PhD**[6], **Kara White Moyes, PhD**[7], **Genta Narazaki, PhD**[3,4], **Koichiro Kuwahara, MD, PhD**[6], **Michael Laflamme, MD, PhD**[7], **Satoshi Matsuoka, MD, PhD**[5], **Norio Nakatsuji, PhD**[8], **Kazuwa Nakao, MD, PhD**[6], **Chulan Kwon, PhD**[1], **David A. Kass, MD**[1], **Felix B. Engel, PhD**[2], and **Jun K. Yamashita, MD, PhD**[3,4]

[1]Division of Cardiology, The Johns Hopkins University School of Medicine, Baltimore, MD

[2]Experimental Renal & Cardiovascular Research, Dept of Nephropathology, Institute of Pathology, University of Erlangen-Nürnberg, Erlangen, Germany

[3]Laboratory of Stem Cell Differentiation, Stem Cell Research Center, Institute for Frontier Medical Sciences, Kyoto University, Kyoto

[4]Dept of Cell Growth & Differentiation, Center for iPS Cell Research & Application, Kyoto University, Kyoto

[5]Dept of Integrative Physiology, Faculty of Medical Sciences, University of Fukui, Fukui

[6]Dept of Medicine & Clinical Science, Kyoto University Graduate School of Medicine, Kyoto, Japan

[7]Dept of Pathology, Center for Cardiovascular Biology, University of Washington, Seattle, WA

[8]Dept of Development & Differentiation, Institute for Frontier Medical Sciences, Kyoto University, Kyoto

Abstract

Background—The proliferation of cardiomyocytes is highly restricted after postnatal maturation, limiting heart regeneration. Elucidation of the regulatory machineries for the proliferation and growth arrest of cardiomyocytes is imperative. Chemical biology is efficient to dissect molecular mechanisms of various cellular events and often provide therapeutic potentials. We have been investigating cardiovascular differentiation with pluripotent stem cells (PSCs). The combination of stem cell and chemical biology can provide novel approaches to investigate the molecular mechanisms and manipulation of cardiomyocyte proliferation.

Methods and Results—To identify chemicals that regulate cardiomyocyte proliferation, we performed a screening of a defined chemical library based on proliferation of mouse PSC-derived cardiomyocytes and identified 4 chemical compound groups - inhibitors of glycogen synthase kinase-3 (GSK3), p38 mitogen-activated protein kinase (MAPK) and Ca^{2+}/calmodulin-dependent protein kinase II (CaMKII), and activators of extracellular signal-regulated kinase (ERK). Several

Correspondence: Hideki Uosaki, MD, PhD, Division of Cardiology, The Johns Hopkins University, School of Medicine, 720 Rutland Ave. Ross 954, Baltimore, MD 21218, Tel: +1-410-512-2154, Fax: +1-410-502-2558, huosaki1@jhmi.edu. Jun K. Yamashita, MD, PhD, Laboratory of Stem Cell Differentiation, Institute for Frontier Medical Sciences, Kyoto University, 53, Shogoin Kawaharacho, Sakyo-ku, Kyoto, 606-8507, Japan, Tel: +81-75-751-3853, Fax: +81-75-751-4824, juny@frontier.kyoto-u.ac.jp.

Conflict of Interest Disclosures: None.

appropriate combinations of chemicals synergistically enhanced proliferation of cardiomyocytes derived from both mouse and human PSCs, notably up to a 14-fold increase in mouse cardiomyocytes. We also examined the effects of identified chemicals on cardiomyocytes in various developmental stages and species. Whereas ERK activators and CaMKII inhibitors showed proliferative effects only on cardiomyocytes in early developmental stages, GSK3 and p38 MAPK inhibitors substantially and synergistically induced reentry and progression of cell cycle in not only neonatal but also adult cardiomyocytes.

Conclusions—Our approach successfully uncovered novel molecular targets and mechanisms controlling cardiomyocyte proliferation in distinct developmental stages and offered PSC-derived cardiomyocytes as a potent tool to explore chemical-based cardiac regenerative strategies.

Keywords

cardiomyocyte; embryonic stem cell; proliferation; small molecules

Life-threatening heart diseases, such as myocardial infarction and heart failure, are major causes of death in developed countries. Due to the almost non-existent cardiomyocyte turnover in the human heart after birth, recovery of cardiac function after heart disease is insufficient.[1–3] The low levels of proliferation and regeneration ability of cardiomyocytes must be overcome to effectively treat these diseases. Although numerous causes of postnatal cell cycle arrest were extensively investigated, such as balances of cyclins, cyclin dependent kinases (CDKs) and CDK inhibitors[4], growth factors[5–9], transcription factors[10–14] and micro RNA[15], heart regenerative medicine has not been effective. One of the limitations is lack of efficient methods for manipulating multiple factors simultaneously.

We hypothesized that a chemical biological approach would be a suitable answer to this problem. Compared to conventional genetic methods, chemical-biological approaches for exploring key biological mechanisms have many advantages, enabling temporal control, rapid inhibition or activation, and regulation of functionally overlapping targets.[16,17] Moreover, chemicals can function across similar species and can be directly applied as therapeutic drugs. Thus, identifying novel chemicals would be an efficient approach to elucidate novel mechanisms regulating cardiomyocyte proliferation and finally employ cardiac regeneration as a therapeutic strategy. Nevertheless, no efficient chemical screening platform for cardiomyocyte proliferation has been explored to date. Recent advances in imaging and analyzing have led to novel approaches to analyze numerous samples automatically. These cell-based and imaging-based methods to screen are called high-content screening (HCS), providing various information on cellular phenotype including cell division.[18]

Pluripotent stem cells (PSCs), including both embryonic stem cells (ESCs) and induced pluripotent stem cells (iPSCs) have great potentials for therapeutic purpose and for drug discovery as they can give rise to any cell types, including cardiomyocytes.[19–23] We have been investigating cardiovascular cell differentiation and regeneration with the use of PSCs, and have established efficient methods for cardiac differentiation from mouse and human PSCs.[24–28] Here we combined our stem cell technology and chemical-biology with HCS to identify chemicals inducing cardiomyocyte proliferation. We successfully identified several chemicals with distinct molecular targets and confirmed their proliferative effects on cardiomyocytes from mouse PSCs. We further demonstrated that the chemical-induced effects on cardiomyocytes from different stages of maturation - embryos, neonates and adults. This study provides novel understanding for molecular machineries and would offer efficient ways to regulate cardiomyocyte proliferation with chemicals.

Methods

Reagents and Antibodies

The SCADS inhibitor kit containing approximately 280 well-established kinase inhibitors[29,30] was a gift from the Screening Committee of Anticancer Drugs supported by a Grant-in-Aid for Scientific Research on Priority Area 'Cancer' from The Ministry of Education, Culture, Sports, Science and Technology, Japan. See Supplemental Methods for reagents and antibodies.

High-Content Screening

The screening process is summarized in Figure S1 and S2. FACS-purified mouse ESC-derived cardiomyocytes (mESCMs) were plated on 0.1% gelatin-coated 96-well plates at 500 cells per well. Cells were treated with chemicals from SCADS inhibitor kit (0.2μM–5μM) for 5 days, followed by fixation and staining with anti-α-myosin heavy chain (αMHC) antibody and DAPI. A DAPI-positive spot in an αMHC-positive area was counted as one nucleus (Figure S2c). αMHC-positive nuclei in four low magnification fields, covering approximately 60% of a single well of 96-well plates, were counted using HCS system ImageXpress (Molecular Devices, Sunnyvale, CA, USA) and image processing software MetaXpress (Molecular Devices).

Statistics

All experiments were repeated at least three times, except the first screen that was repeated twice. Values were reported as mean ± SD and were analyzed by Mann-Whitney test (for two-group comparison), or by Dunn's test (for multiple comparison) using a statistics software, GraphPad Prism (GraphPad Software, Inc., CA, USA). Values of $p < 0.05$ were considered to be statistically significant.

See Supplemental Methods for mouse ESC and human ESC/iPSC culture and differentiation, cardiomyocyte isolation, immunostaining, cell-cycle analysis by flow cytometry, Western blotting, gene knockdown, electrophysiological study, and quantitative reverse transcriptional polymerase chain reaction (qPCR).

Results

Chemical Library Screening for Cardiomyocyte Proliferation in mESCMs

A mouse ESC line carrying αMHC promoter-driven enhanced green fluorescent protein (αMHC-EGFP)[25] was used to prepare purified early differentiated cardiomyocytes (Figure S1), with which we evaluated the chemical-induced effects on cardiomyocyte proliferation. mESCMs appear at 3–4 days after Flk1-positive mesoderm cells were cultured on OP9 stroma cells as we previously reported (Flkd3 to d4; Figure S1).[25,27] Within a few days after the cells differentiated to cardiomyocytes, they ceased their proliferation similar to cardiomyocytes *in vivo*. To screen chemicals that exhibit a direct pro-proliferative effect on mESCMs, we sorted, purified and re-cultured αMHC-EGFP-positive mESCMs at Flkd6 (Figure S2b–d). For the primary screen, we performed HCS to directly count the number of cardiomyocyte nuclei (Figure S2c). Purified mESCMs were re-plated on 96-well plate with treatment of each chemical from the SCADS inhibitor kit in three concentrations (0.2, 1, 5 μM). Five days after treatment (Flkd6+5), the average number of mESCM nuclei was 35.6 ± 17.5 (cells per field, n = 35) in the control condition. Seven chemicals increased mESCM nucleus number more than mean + 2SD of control (red spots in Figure 1a and Table S1). Two Ca^{2+}/calmodulin-dependent kinase II (CaMKII) inhibitors increased the number of mESCM nuclei more than mean + 1SD of control (blue spots in Figure 1a and Table S1).